Transition to Temporal Chaos in an O(2)-Symmetric Convective System for Low Prandtl Numbers

Arantxa ALONSO[*], Juan SÁNCHEZ and Marta NET

Universitat Politècnica de Catalunya, Departament de Física Aplicada, Campus Nord, Mòdul B4, 08034 Barcelona, Spain

Two-dimensional nonlinear convection in a vertical rotating cylindrical annulus with flat adiabatic stress-free lids, heated from the inside and with radial gravity, is numerically analyzed for a low value of the Prandtl number, $\sigma = 0.025$. When the Rayleigh number exceeds a critical value, the conduction state becomes unstable and steady columns parallel to the axis of rotation, and characterized by a finite integer azimuthal wavenumber, n, are the preferred form of convection at the onset for large rotation rates. Despite the presence of rotation, equations retain the $\mathbf{O}(2)$ symmetry for z-independent columnar solutions. Both by using continuation techniques and by a time-integration of the evolution equations, primary nonlinear solutions are obtained for a moderate value of the radius ratio, and are found to give way to periodic solutions in the form of direction reversing travelling waves. The new solution keeps the same wavenumber and breaks the reflection symmetry of the columns. As a consequence, an oscillatory mean flux appears that decreases the efficiency of the heat transport in the radial direction. By further increasing the Rayleigh number, a transition from the oscillatory to a chaotic flow takes place. This chaotic state is reached via a pitchfork bifurcation that breaks the rotation symmetry $\mathbf{R}_{2\pi/3}$ of the orbit, followed by a subcritical Neimark-Sacker bifurcation that gives rise to a quasi-periodic solution. Finally, the invariant torus breaks up and a chaotic regime appears.

§1. Introduction

Geophysical and astrophysical processes, such as fluid motions in the atmospheres of major planets and in planetary fluid cores, have motivated numerous studies of thermal convection in rotating systems. These large-scale motions, which are driven by temperature gradients, all have in common the spherical geometry of the convective shell, on one hand, and the strong effect of rotation in the convective system, on the other. The key role played by the Coriolis force makes the dynamics of rotating systems surprisingly different from that of the nonrotating ones.

A global study of these phenomena using models that realistically reproduce the conditions of the physical system is unapproachable. One of the main difficulties arises from the spherical geometry, which makes the orientation of gravity and rotation vary with latitude. This fact leads to expensive fully three-dimensional computations; it makes linear and weakly nonlinear analytical solutions very hard to obtain and experimental studies difficult to carry out, since such a convective system is extremely complicated to reproduce in the laboratory due to the presence of vertical gravity. In spite of these difficulties, some numerical works dealing with spherical convection have been done during the last decade (see, for instance, [1] and [2]), though they are limitted to some particular aspects of the dynamics. It is thus desirable

---

[*] E-mail address: arantxa@fa.upc.es

to consider simpler convection systems that provide a better understanding of the nature of instabilities in rotating systems.

The dynamics in rotating convective systems is mainly influenced by the relative orientation of gravity, temperature gradient and rotation vectors. In the case that the three vectors are parallel, some of the most extensively studied systems are those formed by a rotating plane layer or a vertical cylinder heated from below, which are used as a model of convection in high latitudes of spherical shells. For other latitudes, among the systems in which gravity, temperature gradient and rotation do not have the same direction, much attention has been paid to thermal convection driven by radial heating in an annulus rotating uniformly about its axis, and to β-plane convection. The dynamics resulting from a destabilizing thermal gradient perpendicular to rotation depends fundamentally on the direction of gravity.

In the present paper, we consider a convective system formed by a cylindrical annulus rotating about its axis of symmetry with radial gravity and outwards heating, which is an example of a barotropic problem. In a previous work, the linear stability of the conduction state, either with stress-free [3] and no-slip [4] boundary conditions for the velocity on the lids of the annulus, was studied. It was shown that in the first case there is always a moderate rotation rate above which steady z-independent two-dimensional columns parallel to the axis of rotation are the preferred solutions at the onset of convection. These solutions are characterized by a fixed azimuthal wavenumber determined by the radius ratio of the annulus. For large rotation rates, a geostrophic balance is achieved in this regime, with the Coriolis force being exactly balanced by a pressure gradient, and the solution is known as *Taylor columns*. When no-slip boundary conditions are considered, convection is found to be nearly two-dimensional, with departures from two-dimensionality confined to narrow layers at the ends of the annulus in the limit of rapid rotation, and the pattern slightly drifts. Similar results have been obtained in the case of an annulus heated by a uniform distribution of heat sources [5], [6]. The present study will focus on the nonlinear analysis of this z-independent columnar solution obtained in the stress-free case.

Since the constraint of rotation forces the motion to remain two-dimensional, we have studied numerically the stability of the Taylor columns by considering perturbations independent of the axial coordinate. Indeed, there is experimental evidence that the two-dimensional nature of the columns is preserved up to large Rayleigh numbers for large rotation rates [7]. A study of the nonlinear regime in a low rotating annulus should include three-dimensional disturbances, since they will very probably dominate the dynamics of the system, as can be inferred from the stability analysis of a two-dimensional solution in a low rotating annulus in the limit $\eta \to 1$ considered in [8]. Both the results obtained by a weakly nonlinear analysis based on amplitude equations, and the numerical results show that the convection rolls become unstable, giving rise to a three-dimensional structure after either a *cross-roll* or a subharmonic *varicose* instability takes place.

Moreover, the problem of the stability of the two-dimensional columns in a rotating annulus provides a simple fluid dynamic system which is highly attractive from the point of view of bifurcation theory, as the undergoing bifurcations can be described in terms of symmetry breaking instabilities. Although the rotation

of the annulus breaks the reflection symmetry, turning the $\mathbf{O}(2)$ symmetry of the nonrotating annulus into a $\mathbf{SO}(2)$ symmetry [9], when the two-dimensional solution is considered, equations retrieve the reflection invariance and the system becomes $\mathbf{O}(2)$-symmetric. Symmetries affect the nature of instabilities in a system. The type of secondary bifurcations that a solution which has broken the rotation symmetry in a $\mathbf{O}(2)$-symmetric system may undergo is known. If the azimuthal structure of the primary flux is mantained, according to bifurcation theory [10], [11] there are four possible codimension one secondary bifurcations. The new solution can either keep the reflection symmetry of the basic solution or break it. In the first case, the bifurcation can be a saddle-node or a Hopf bifurcation, giving rise to an exchange of stabilities or to a standing wave without any spatial drift. In the second case, it can either be a pitchfork or a Hopf bifurcation, leading to travelling waves, which have a drift speed that increases with increasing bifurcation parameter, or to direction reversing travelling waves, a pattern that alternatively drifts back and forth [12]. Obviously, if the secondary solution changes the wavenumber of the primary flux the type of generic secondary bifurcation and the transition to chaos can be different.

The remainder of the paper is organized as follows. After presenting the mathematical formulation of the problem and describing the numerical techniques used to solve it in Sec. 2, the results are presented and discussed in Sec. 3 for a low value of the Prandtl number, $\sigma = 0.025$. The onset of the first instability and the secondary solutions in the form of direction reversing travelling waves are analyzed in 3.1, while the transition route to chaos exhibited by the system is detailed in 3.2.

§2.   Mathematical formulation and numerical methods

We consider the problem of nonlinear convection in a cylindrical annulus of radius ratio $\eta = r_i/r_o$, where r_i and r_o are the inner and outer radii, rotating about its axis of symmetry, filled with a Boussinesq fluid of thermal diffusivity κ, thermal expansion coefficient α and kinematic viscosity ν. The inner and outer sidewalls are mantained at constant temperatures T_i and T_o, with $T_i > T_o$, and the gravitational acceleration is taken radially inwards, $\mathbf{g} = -g\hat{\mathbf{e}}_r$, and is assumed to be constant. With upper and lower horizontal boundaries, there exists a basic conduction state

$$T_c(r) = T_i + \Delta T \frac{\ln r/r_i}{\ln \eta}, \qquad (2\cdot1)$$

with $\Delta T \equiv T_i - T_o$, in which heat is radially transferred towards the outer cylinder by thermal conduction without macroscopic motions of the fluid. The stability of the conduction state is described by the Navier-Stokes continuity and heat equations which, once nondimensionalized by using the gap width $d = r_o - r_i$ as lengthscale, d^2/κ as timescale and ΔT as temperature scale, take the form

$$\sigma^{-1}\left(\partial_t \mathbf{u} + (\mathbf{u} \cdot \nabla)\mathbf{u}\right) = -\nabla p + \nabla^2 \mathbf{u} + Ra\Theta\hat{\mathbf{e}}_r - Ta^{1/2}\hat{\mathbf{e}}_z \times \mathbf{u}, \qquad (2\cdot2a)$$

$$\nabla \cdot \mathbf{u} = 0, \qquad (2\cdot2b)$$

$$\partial_t \Theta + \mathbf{u} \cdot \nabla \Theta = -\frac{u}{r \ln \eta} + \nabla^2 \Theta. \qquad (2\cdot2c)$$

Here, $\mathbf{u} = (u, v, w)$ is the velocity field in cylindrical coordinates and Θ denotes the departure of the temperature from its conduction profile, $T = \Theta + T_c$. The Rayleigh, Prandtl and Taylor numbers are defined by

$$Ra = \frac{\alpha \Delta T g d^3}{\kappa \nu}, \qquad \sigma = \frac{\nu}{\kappa}, \qquad Ta = 4\left(\frac{\Omega}{\nu/d^2}\right)^2.$$

The presence of the Coriolis term in the equations breaks the reflection symmetry in any vertical plane containing the axis of rotation, $\mathbf{R}_1$. Therefore, the rotating cylindrical annulus is invariant under rotations, $\mathbf{R}_\theta$, and under reflections in the equatorial plane, $\mathbf{R}_3$, its group of symmetry being $\mathbf{SO}(2) \times \mathbf{Z}_2$, where $\mathbf{SO}(2)$ is the group of rotations around the z-axis and $\mathbf{Z}_2$ the group generated by $\mathbf{R}_3$, while the symmetry of the nonrotating annulus is $\mathbf{O}(2) \times \mathbf{Z}_2$, where $\mathbf{O}(2)$ is the group generated by rotations around the z-axis and the reflections $\mathbf{R}_1$.

We are interested in studying the nonlinear evolution of the two-dimensional solution. For this $z-$independent solution there is no vertical velocity, $w = 0$. The Coriolis term can be written as a gradient and introduced in the pressure term, and the equations reduce to

$$\partial_t u = -\partial_r p + \sigma\left[\nabla^2 \mathbf{u}\right]_r + \sigma Ra\Theta - \left[(\mathbf{u} \cdot \nabla)\mathbf{u}\right]_r, \qquad (2 \cdot 3a)$$

$$\partial_t v = -\frac{1}{r}\partial_\theta p + \sigma\left[\nabla^2 \mathbf{u}\right]_\theta - \left[(\mathbf{u} \cdot \nabla)\mathbf{u}\right]_\theta, \qquad (2 \cdot 3b)$$

$$\partial_t \Theta = \nabla^2 \Theta - \frac{u}{r \ln \eta} - \mathbf{u} \cdot \nabla\Theta, \qquad (2 \cdot 3c)$$

$$\nabla \cdot \mathbf{u} = 0. \qquad (2 \cdot 3d)$$

They will be solved with no-slip and perfectly conducting boundary conditions

$$\mathbf{u} = \theta = 0 \qquad (2 \cdot 4)$$

on the lateral walls, $r_i = \eta/(1-\eta)$ and $r_o = 1/(1-\eta)$. It is important to notice that, due to the absence of the Coriolis term, equations (2·3) become invariant under reflections in vertical planes. So, when the columnar solution is considered, the system retrieves the $\mathbf{O}(2)$ symmetry of the nonrotating annulus.

To integrate the nonlinear equations, we have developed a semi-implicit time-splitting spectral code which allows us to find any time-dependent stable solution of the system in an efficient way. In particular, following [13], we have used a mixed stiffly-stable second order time-accurate scheme, implicit for the linear terms and explicit for the nonlinear terms. The variables have been expanded in terms of Chebyshev polinomials, $T_l(r)$, for the radial dependence, and Fourier expansions for the periodic direction

$$u(r, \theta, t) = \sum_{l,n} u_{l,n}(t) T_l(r) e^{in\theta}.$$

An improved boundary condition has been introduced to minimize the effect of erroneous numerical boundary layers induced by splitting methods [13]. The details can be found in [14].

The study of the dynamics has been completed with the use of a continuation code [15] in order to find the stationary nonlinear columns when any parameter of interest, such as the Rayleigh number, is varied. It is possible to follow any stationary branch of solutions with a high precision, even if they are unstable, and to locate the different bifurcations that occur. In this case, to solve the equations we have used a technique based on velocity potencials. As in the time integration scheme, the variables have been expanded in terms of Chebyshev polynomials and Fourier expansions. In this formulation the velocity field is written as

$$\mathbf{u} = f\hat{\mathbf{e}}_\theta + \nabla \times \Psi\hat{\mathbf{e}}_z,$$

where $\Psi = \Psi(r,\theta)$ is the streamfunction, which does not contain the zero-mode in the Fourier expansion, and $f = f(r)$ is related with the $n = 0$ mode. The nonlinear equations to be solved are

$$\partial_t f = \sigma\nabla_-^2 f + P_\theta\left[\nabla_h^2\Psi\left(\frac{1}{r}\partial_\theta\Psi\right)\right], \tag{2·5a}$$

$$\partial_t\nabla_h^2\Psi = \sigma\nabla_h^4\Psi + (1 - P_\theta)\frac{\sigma Ra}{r}\partial_\theta\Theta + (1 - P_\theta)J(\Psi, \nabla_h^2\Psi) + \tag{2·5b}$$

$$+\nabla_-^2 f\left(\frac{1}{r}\partial_\theta\Psi\right) - f\left(\frac{1}{r}\partial_\theta\nabla_h^2\Psi\right), \tag{2·5c}$$

$$\partial_t\Theta = \nabla_h^2\Theta - \frac{1}{r^2\ln\eta}\partial_\theta\Psi + J(\Psi, \Theta) - f\left(\frac{1}{r}\partial_\theta\Theta\right), \tag{2·5d}$$

where $\nabla_-^2 = \partial_r(\partial_r + 1/r)$. P_θ is the projection operator that extracts the zero-mode in a Fourier expansion,

$$P_\theta F = \frac{1}{2\pi}\int_0^{2\pi} F(r, \theta, z, t)d\theta,$$

and J is the jacobian in cylindrical coordinates.

§3. Numerical results and discussion

The results we are going to present have been obtained with a moderate value of the radius ratio, $\eta = 0.3$. As for the value of the Prandtl number of the fluid, which is expected to influence greatly the nonlinear behaviour, we have chosen $\sigma = 0.025$, the Prandtl number of mercury.

3.1. *Primary nonlinear solutions and secondary bifurcation*

As a first step, we have carefully checked both the continuation and time-integration codes, which reproduce accurately the supercritical pitchfork bifurcation of the system. Irrespective of the value of the Prandtl number, the primary bifurcation takes place at a critical Rayleigh number $Ra_c^1 = 1799.8$, and the most unstable mode at the onset of convection is characterized by an azimuthal wavenumber $n = 3$. This primary flux, which is a nonaxisymmetric solution, breaks the rotation symmetry, $\mathbf{R}_\theta$, of the basic state but, as it is invariant under reflections in vertical planes

between the columns, $\mathbf{R}_1$, and under the rotation $\mathbf{R}_{2\pi/3}$, its symmetry group is $\mathbf{D}_3$. Figure 1 shows the streamfunction and the Fourier coefficients averaged in the radial direction for a nonlinear column.
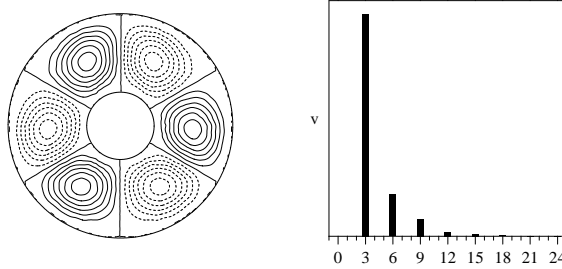

Fig. 1. Steady nonlinear column. The contour plot represents the streamfunction and the bar chart shows the Fourier coefficients of the azimuthal velocity averaged in the radial direction. $Ra = 2500$.

Once the nonlinear steady columns bifurcating from the conduction state have been computed, the critical Rayleigh number for which these columns become unstable and the character of the secondary bifurcation must be determined. The numerical linear stability analysis of the columnar solution shows that a secondary Hopf bifurcation takes place at a Rayleigh number $Ra_c^2 = 4114$, the imaginary part of the critical eigenvalue being $\lambda_I = \pm 23.5$. The nonlinear steady columns become unstable and they are found to give rise to direction reversing travelling waves (DRTW), which is a pattern that alternatively drifts back and forth in the azimuthal direction. The new solution keeps the same azimuthal wavenumber of the steady columns, $n = 3$, and is characterized by the appearance of a mean flow in the azimuthal direction that breaks the reflection symmetry of the columns.

Figure 2 shows the change in the structure of the columns after the secondary bifurcation. Close to the bifurcation point, the pattern oscillates back and forth with a frequency given by the imaginary part of the eigenvalue whose real part becomes zero. The oscillation in the azimuthal direction can be appreciated in the shadowgraph (right), which represents the evolution in time (y-axis) of temperature and its θ-dependence (x-axis). Clearly, the DRTW breaks the reflection symmetry with respect to vertical planes between the columns. The bar chart (lower-left) corresponds to the Fourier spectrum of the azimuthal velocity, v, averaged in the radial direction. After the bifurcation, the θ-independent mode of v, f, begins to contribute to the solution. The dependence of f (mean flow) on the radial coordinate, x, in four time instants, $t = 0, T/4, T/2, 3T/4$, is also shown in the figure (top-left). As the area enclosed by each curve equals the instant net mass flow, it can be inferred from the plot that there exists an oscillatory mass transport in the azimuthal direction. That is, the instant net mass flow is non-zero, though it vanishes when averaged in a whole period.

Figure 3 shows the dependence of the Nusselt number, averaged in time for the periodic solution, on the Rayleigh number. In our problem, the Nusselt number is a measure of the radial heat transport by convection, and has been computed in the outer cylinder. After the secondary bifurcation, there is a significant decrease in
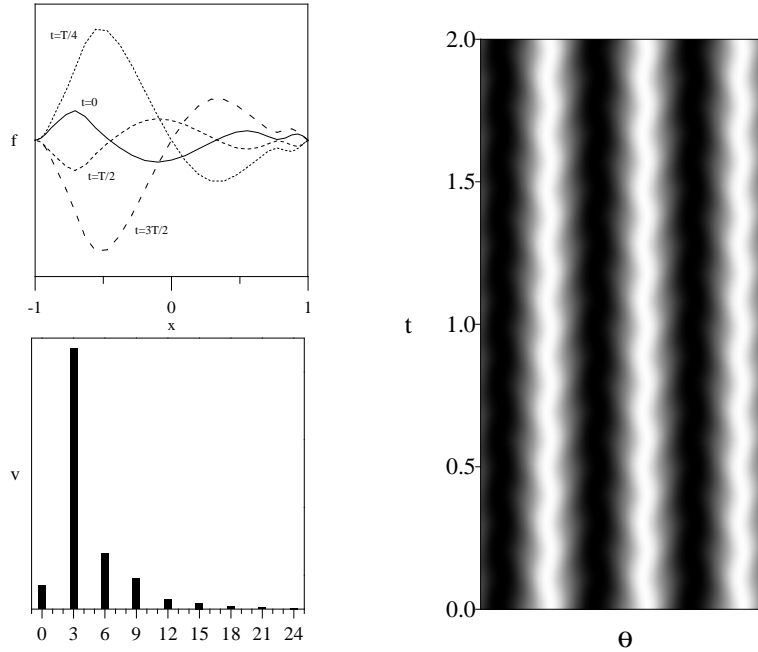
Fig. 2. Direction reversing travelling wave. (top-left) Four snapshots showing the radial dependence of the $n = 0$ mode of the azimuthal velocity, f (mean flow). (lower-left) Fourier coeficients averaged in the radial direction. (right) Shadowgraph showing the evolution of temperature in time for a fixed value of the radial coordinate, $r = (r_1 + r_2)/2$. $Ra = 5000$.

the slope of the curve. This decrease in the efficiency in the radial heat transport is caused by the appearance of the oscillatory mass flow in the azimuthal direction.

The frequency of any periodic solution far from the bifurcation point can be precisely determined by computing the Fourier spectra of the time series. It is obtained that the value of the frequency grows as the Rayleigh number increases. Just in the bifurcation point, for a Rayleigh number $Ra = 4114$, the frequency is $f = 3.74$, while for a Rayleigh number $Ra = 6500$, the Fourier spectrum shows that the solution still remains periodic, the frequency of oscillation being $f = 5.15$.

3.2. *Transition to a chaotic regime*

As can be seen in figures 1 and 2, the Taylor columns and the DRTW preserve the $\mathbf{Z}_3$ invariance imposed by the chosen radius ratio, $\mathbf{Z}_3$ being the cyclic group generated by the rotation $\mathbf{R}_{2\pi/3}$. Moreover, the periodic solution is an S-cycle, i.e. applying a reflection to the solution equals an evolution in time of $T/2$, so only the multipliers $\mu = 1$ and $\mu = e^{\pm i\theta_0}$ of the associated Poincaré map can appear (see [16] for details). Between $Ra = 6950$ and $Ra = 7000$ a tertiary spatial subharmonic bifurcation is identified in the system. We have carefully checked that at the tertiary bifurcation there is no new frequency appearing in the Fourier spectra of the time series, so

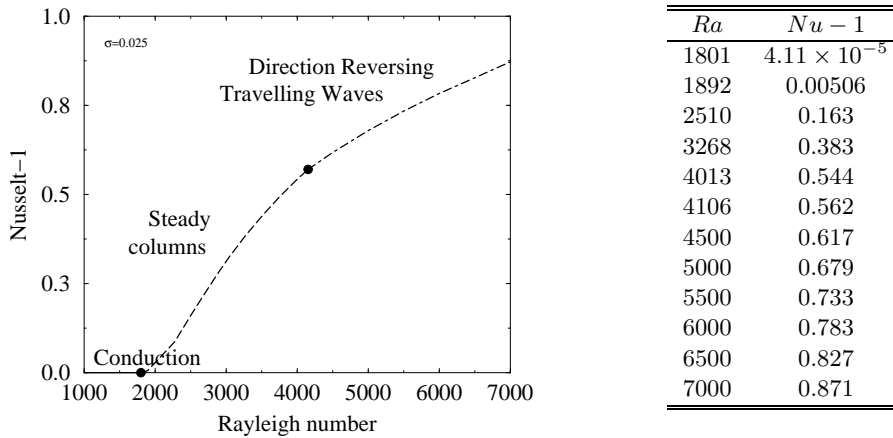| Ra	$Nu - 1$
1801	4.11×10^{-5}
1892	0.00506
2510	0.163
3268	0.383
4013	0.544
4106	0.562
4500	0.617
5000	0.679
5500	0.733
6000	0.783
6500	0.827
7000	0.871

Fig. 3. (left) Nusselt number as a function of the Rayleigh number and (right) numerical values of the Nusselt number corresponding to some steady and periodic solutions.

the new solution remains periodic and, accordingly, the unit circle is crossed by the real multiplier. Figure 4 displays the new periodic orbit very far from transition, for $Ra = 12300$. The bar charts show that although the main wavenumber $n = 3$ and its harmonics are still dominant, all the modes are now nonzero. The shadowgraph of the temperature at a fixed radius clearly proves that, as a result, the spatial $\mathbf{Z}_3$ invariance of the columns is broken. The new pattern of convection consists of three oscillating columns like those in the DRTW, but with a different waveform, amplitude and phase. The waveform is nearly the same in two of them, but the third one is meandering. A similar cell pattern can be found when a fixed point bifurcates with trihedral $\mathbf{D}_3$ symmetry (see [17]). In our case, however, the phase shifts from one to the next are not exactly $2\pi/3$ or π.

When $Ra = 12330$, the system undergoes a fourth bifurcation. The Poincaré section of figure 5 (right) shows that an invariant two-dimensional torus appears through a subcritical Neimark-Sacker bifurcation. It can be inferred from the Fourier spectrum of the time series corresponding to the Nusselt number included in figure 5 (left) that the new frequency in the system is very small, $f_2 = 0.815$, in comparison with the value of the main one, $f_1 = 14.519$. Notice that the main frequency f_1 associated to the time series of the Nusselt number is twice the frequency of the velocity field because this number is an azimuthal average of a temperature that bifurcates from an S-cycle.

The quasi-periodic solution turns out to be stable in a small interval of the control parameter. A moderate increment in the Rayleigh number produces a great change in the dynamics of the system, the solution being already chaotic for a Rayleigh number $Ra = 12000$. The Fourier spectrum of the time series of the solution and its Poincaré section indicate that the bifurcation giving rise to this regime introduces another frequency in the system. Chaos is thus probably reached after five bifurcations, four of them well described in literature.
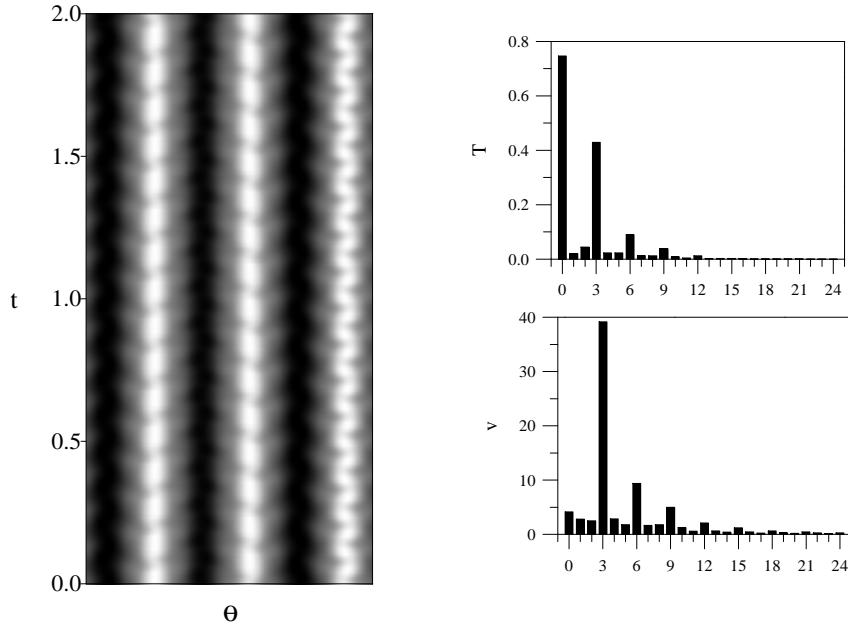
Fig. 4. (left) Shadowgraph showing the evolution of temperature in time (y-axis) for a fixed
value of the radial coordinate, $r = (r_1 + r_2)/2$, and (right) azimuthal spectra of temper-
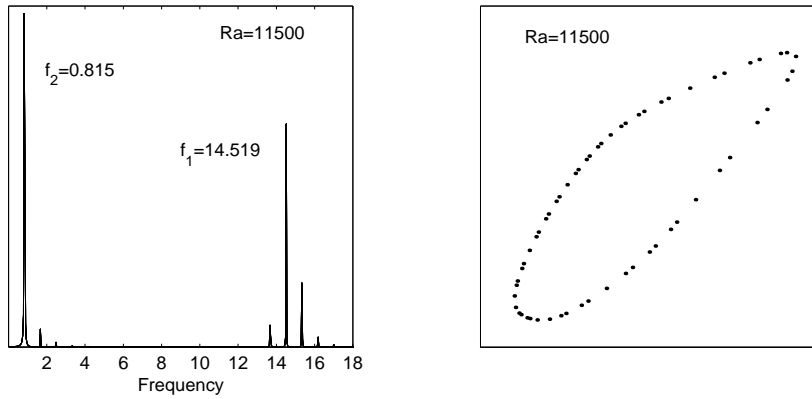ature, T, and azimuthal velocity, v, for a solution corresponding to $Ra = 12300$.

Fig. 5. (left) Fourier spectrum of the temporal series and (right) Poincaré section of the
quasi-periodic orbit. The solution corresponds to $Ra = 11500$.

The transition route to chaos that this convective system exhibits depends
strongly on the Prandtl number. Although all the results presented in this paper
correspond to a low value of the Prandtl number, $\sigma = 0.025$, for which the momen-
tum advection term plays an important role, preliminary results for moderate and
high values of σ confirm that there is a drastic change in the nature of the secondary
bifurcation when the Prandtl number is increased. A steady pitchfork bifurcation
that changes the spatial periodicity of the basic column takes place in the system, the

pattern that arises after the secondary bifurcation no longer being time-dependent. Furthermore, this bifurcation is detected for a much higher Rayleigh number.

Nevertheless, steady-state pitchfork bifurcations of the type obtained for a large value of the Prandtl number are also identified in the $\sigma = 0.025$ case when the unstable branches that bifurcate from the conduction state are analyzed. From the unstable branch corresponding to a steady $n = 2$ column, several subharmonic solutions that also remain unstable are found to arise after pitchfork bifurcations take place in the system. The importance of not leaving aside the study of the unstable branches to fully determine the dynamics of the system should be emphasized. The subsequent bifurcations in these branches may lead to the stabilization of solutions that coexist with the main stable branch, and this is indeed the case in our problem. A steady stable $n = 4$ branch of solutions that coexists with the $n = 3$ DRTW appears in the system as a result of a strong spatial interaction of the $n = 2$ and $n = 4$ modes. The detailed description of this 1:2 resonance will be pursued in the near future.

Acknowledgements

References

1) K. Zhang, J. Fluid Mech. **236** (1992), 535.
2) A. Tilgner and F.H. Busse, J. Fluid Mech. **332** (1997), 359.
3) A. Alonso, M. Net and E. Knobloch, Phys. Fluids **7**(5) (1995), 935.
4) A. Alonso, M. Net, I. Mercader and E. Knobloch, Fluid Dynamics Research **24** (1999), 133.
5) G.T. Greed and K. Zhang, Geophys. Astrophys. Fluid Dynamics **82** (1996), 23.
6) K. Zhang and G.T. Greed, Phys. Fluids **10**(9) (1998), 2396.
7) M.A. Azouni, E.W. Bolton and F.H. Busse, Geophys. Astrophys. Fluid Dynamics **34** (1986), 301.
8) M. Auer, F.H. Busse and R.M. Clever, J. Fluid Mech. **97** (1991), 414.
9) E. Knobloch, *Lectures on Solar and Planetary Dynamos* (ed. M.R.E. Proctor and A.D. Gilbert, Cambridge University Press, 1994), p. 331.
10) M. Golubitsky and D.G. Schaeffer, *Singularities and Groups in Bifurcation Theory (vol. I)* (Springer-Verlag, New York, 1985).
11) E. Knobloch, Phys. Fluids **8**(6) (1996), 1446.
12) A.S. Landsberg and E. Knobloch, Phys. Lett. A **159** (1991), 17.
13) G.E. Karniadakis, M. Israeli and S.A. Orszag, Journal of Computational Physics **97** (1991), 414.
14) A. Alonso, PhD thesis, Universidad Politécnica de Cataluña (1999).
15) J. Sánchez, PhD thesis, Universidad de Barcelona (1994).
16) Y.A. Kuznetsov, *Elements of Applied Bifurcation Theory* (Springer-Verlag, New York, 1998).
17) M. Golubitsky, I. Stewart and D.G. Schaeffer, *Singularities and Groups in Bifurcation Theory (vol. II)* (Springer-Verlag, New York, 1985).